



Gap opening in graphene by shear strain

Giulio Cocco, Emiliano Cadelano, and Luciano Colombo*

Department of Physics, University of Cagliari, Cittadella Universitaria, Monserrato, I-09042 Cagliari, Italy
(Received 2 April 2010; revised manuscript received 1 June 2010; published 22 June 2010)

We exploit the concept of strain-induced band-structure engineering in graphene through the calculation of its electronic properties under uniaxial, shear, and combined uniaxial-shear deformations. We show that by combining shear deformations to uniaxial strains it is possible to modulate the graphene energy-gap value from zero up to 0.9 eV. Interestingly enough, the use of a shear component allows for a gap opening at moderate absolute deformation, safely smaller than the graphene failure strain.

DOI: [10.1103/PhysRevB.81.241412](https://doi.org/10.1103/PhysRevB.81.241412)

PACS number(s): 73.22.Pr, 81.05.ue, 62.25.-g

Graphene exhibits a number of exotic electronic properties, such as unconventional integer quantum Hall effect, ultrahigh electron mobility, electron-hole symmetry, and ballistic transport even at room temperature.¹⁻³ Full account of these features is provided by the relativistic Dirac theory⁴ suitably developed within the standard condensed-matter formalism. A key feature of graphene is that its electronic density of states (DOS) vanishes at the so-called Dirac points, where the valence and the conduction bands (CBs) cross with a linear energy-momentum dispersion. Due to the hexagonal symmetry of graphene, the Dirac points are located at two high-symmetry points of its Brillouin zone (BZ).

While many other properties of graphene are very promising for nanoelectronics, its zero-gap semiconductor nature is detrimental, since it prevents the pinch off of charge current as requested in conventional electronic devices. Different attempts have been therefore tried in order to induce a gap, for instance by quantum confinement of electrons and holes in graphene nanoribbons⁵ or quantum dots.⁶ These patterning techniques are unfortunately affected by the edge roughness problem,⁷ namely, the edges are extensively damaged and the resulting lattice disorder can even suppress the efficient charge transport. The sensitivity to the edge structure has been demonstrated through explicit calculations of the electronic states in ribbons.⁸ More recently, it has been shown experimentally that a band gap as large as 0.45 eV can be opened if a graphene sheet is placed on an Ir(111) substrate and exposed to patterned hydrogen adsorption.⁹

Alternatively, an electronic band gap can be obtained by growing graphene sheets on an appropriately chosen substrate, inducing a strain field controllable by temperature.¹⁰⁻¹³ Recently, it has been experimentally shown that by using flexible substrates a reversible and controlled strain up to $\sim 18\%$ (Ref. 12) can be generated with measurable variations in the optical, phonon, and electronic properties of graphene.¹³ This interesting result suggests that gap opening could be engineered by strain, rather than by patterning. The idea has been theoretically validated by Pereira and Castro Neto¹⁴ showing that a gap is indeed generated by applying an uniaxial strain as large as $\sim 23\%$, approaching the graphene failure strain $\epsilon_f = 25\%$.^{15,16} This large value stands for the high robustness of the gapless feature of graphene under deformation. The same authors propose an alternative origami technique¹⁷ aimed at generating local strain profiles by means of appropriate geometrical patterns

in the substrate, rather than by applying strain directly to the graphene sheet.

In this work, we further develop the above concept of strain engineering by showing how a combination of shear and uniaxial strain can be used to open a gap in a range of reversible and more easily accessible deformations, ranging in between 12% and 17%. We also discuss the merging of Dirac points,¹⁸ which is involved into the gap opening process.

The electronic structure of graphene has been computed for each deformed configuration by means of a semiempirical sp^3 tight-binding (TB) model, making use of the two-center parameterization by Xu *et al.*¹⁹ Despite its semiempirical character, the present TB model correctly provides the occurrence of Dirac points in the band structure of graphene in its equilibrium geometry. Furthermore, the Xu *et al.* parametrization provides accurate scaling functions for the variation in the TB hopping integrals upon lattice distortions. This feature is instrumental for investigating gap opening in graphene by strain. The reliability of the present TB model in describing the strain-related features of graphene has been recently established.^{16,20}

Graphene is a hexagonal lattice with two carbon atoms per unit cell and a lattice basis defined by the vectors (\vec{a}_1, \vec{a}_2) , as shown in Fig. 1, with a nearest-neighbor carbon-carbon distance as small as $a_0 = 1.42 \text{ \AA}$. The in-plane elastic behavior of the honeycomb lattice is isotropic in the linear regime but two inequivalent crystallographic directions can be nevertheless defined: the so-called armchair and zigzag direc-

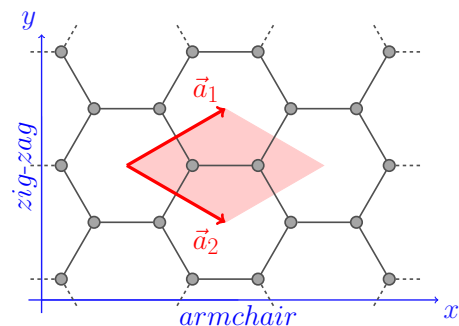


FIG. 1. (Color online) Top view of the hexagonal graphene lattice with its lattice vectors $\vec{a}_{1,2} = a_0(\frac{3}{2}, \pm\frac{\sqrt{3}}{2})$, where a_0 is the equilibrium C-C distance. Axes x and y correspond to the armchair and zigzag directions, respectively. Shaded area represents the unit cell.

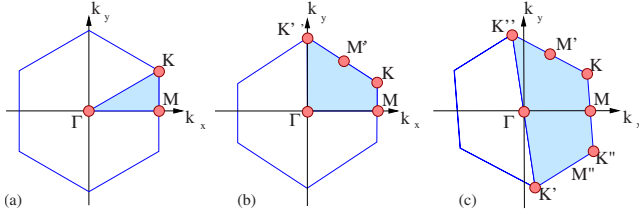


FIG. 2. (Color online) Brillouin zone of graphene under strain. The shaded areas are the corresponding irreducible part: (a) undeformed BZ with $6/mmm$ hexagonal symmetries; (b) BZ deformed by uniaxial strain with mmm rhombic symmetry; and (c) BZ deformed by shear strain with $2/m$ monoclinic symmetry.

tions, shown in Fig. 1 as x and y axes, respectively. According to the Cauchy-Born rule, when straining a graphene sample its lattice vectors are affected accordingly, as well as the associated reciprocal vectors (\vec{b}_1, \vec{b}_2). The deformed vectors are given by $a'_i = (\varepsilon_{ij}a_j + \delta_{ij}a_j)$, where $\hat{\varepsilon} = \{\varepsilon_{ij}\}$ is the strain tensor describing the deformation and $i, j = x, y$. The condition $\vec{a}'_k \cdot \vec{b}'_l = 2\pi\delta_{kl}$ (where $k, l = 1, 2$) allows one to obtain the deformed reciprocal-lattice vectors.

The following in-plane deformations have been applied to the equilibrium honeycomb lattice under plane-strain border conditions:¹⁶ (i) an uniaxial deformation ζ along the armchair direction, corresponding to a strain tensor $\varepsilon_{ij}^{(ac)} = \zeta\delta_{ix}\delta_{jx}$; (ii) an uniaxial deformation ζ along the zigzag direction, corresponding to a strain tensor $\varepsilon_{ij}^{(zz)} = \zeta\delta_{iy}\delta_{jy}$; (iii) an hydrostatic planar deformation ζ , corresponding to the strain tensor $\varepsilon_{ij}^{(p)} = \zeta\delta_{ij}$; (iv) a shear deformation ζ , corresponding to an in-plane strain tensor $\varepsilon_{ij}^{(s)} = \zeta(\delta_{ix}\delta_{jy} + \delta_{iy}\delta_{jx})$.

In order to extend the reliability of the present model to electronic features under strain, our results about the effects of hydrostatic and uniaxial deformations on the band structure are at first compared with previous data available in literature. For graphene under in-plane hydrostatic deformation with $\zeta \leq 15\%$, both in compression and in traction, we have calculated the band electronic structure and the density of states. Since the hydrostatic strain does not change the $D_{6h}(6/mmm)$ symmetry of the hexagonal lattice [Fig. 2(a)], we only observe the variation in the pseudogaps at Γ and M points while the location of the Dirac points is clamped at the K point. In particular, the pseudogap at M decreases almost linearly from 6 eV (for $\zeta = -15\%$) to 1.8 eV (for $\zeta = +15\%$). We remind that its value for the unstrained configuration is 2.2 eV. These results are in quantitative good agreement with Ref. 21. Any other nonhydrostatic deformation lowers the symmetry of the graphene lattice. When an uniaxial strain is applied, all the sixfold and threefold rotational symmetries are lost: a transition from the hexagonal $D_{6h}(6/mmm)$ to the rhombic $D_{2h}(mmm)$ symmetry is observed [Fig. 2(b)]. The irreducible part of the first BZ is also affected by such deformations since its original triangular shape [Fig. 2(a)] is varied to the polygonal form represented in Fig. 2(b). The top of the valence band (VB) and the bottom of the conduction band are shown in Fig. 3 for the undeformed configuration (panel a), as well as under uniaxial deformation (panels b and c, corresponding to a strain $\zeta = 15\%$ along the armchair direction and in the zigzag direction, respectively). The main effect of strain is the opening of a pseudogap at K and K' .

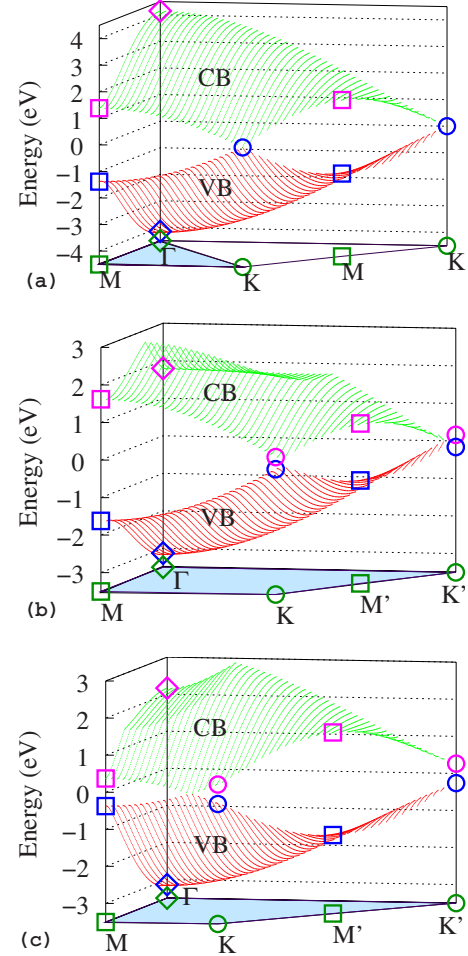


FIG. 3. (Color online) Top of the valence band (red, marked as VB) and bottom of the conduction band (green, marked as CB) of graphene under uniaxial strain. Panel a: band structure of the undeformed lattice. Panels b and c: band structure under uniaxial strain along the armchair and the zigzag directions, respectively. Symbols connect the high-symmetry points of the BZ (bottom shaded area) to the energy of the corresponding electronic states.

Accordingly, the Dirac points are no more located at such high-symmetry points; rather, they drift away within the BZ, either for deformations along armchair direction or along zigzag one. Once again this important qualitative feature is in good agreement with Ref. 14.

Let us now consider the case of an in-plane shear deformation, described by the following shear strain:

$$\hat{\varepsilon} = \begin{pmatrix} 0 & \zeta \\ \zeta & 0 \end{pmatrix}, \quad (1)$$

where ζ is the strain parameter. Such a deformation modifies the original reciprocal-lattice vectors \vec{b}_1 and \vec{b}_2 into

$$\vec{b}'_1 = \frac{2\pi}{a_o} (1 + \zeta^2)^{-1} \left(\frac{1}{3} - \frac{\sqrt{3}}{3}\zeta, \frac{\sqrt{3}}{3} - \frac{1}{3}\zeta \right),$$

$$\vec{b}'_2 = \frac{2\pi}{a_o} (1 + \zeta^2)^{-1} \left(-\frac{1}{3} - \frac{\sqrt{3}}{3}\zeta, -\frac{\sqrt{3}}{3} - \frac{1}{3}\zeta \right). \quad (2)$$

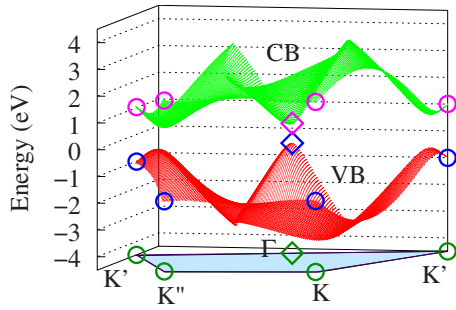


FIG. 4. (Color online) Top of the valence band (red, marked as VB) and bottom of the conduction band (green, marked as CB) of graphene under pure shear strain with $\zeta=20\%$. Symbols connect the high-symmetry points of the BZ (bottom shaded area) to the energy of the corresponding electronic states.

By applying the shear strain given in Eq. (1) to the graphene lattice, its symmetry class is further lowered to monoclinic. The corresponding symmetry group is $2/m$. Because of this change in symmetry, the irreducible part of the BZ is affected accordingly as shown in Fig. 2(c), which has K' , K , K'' , and K' as corners. In the undeformed lattice, a Dirac point is located at each of these corners. The scenario under shear strain is quite different from the case of uniaxial deformations: at the comparatively small strain $\zeta \approx 16\%$, a gap is indeed opened. The rise of a gap in the electronic band structure under shear is due to a peculiar process that involves the merging²² of two Dirac points, namely, D' and D'' , which move away from the corners K' and K' and approach each other inside the BZ.

It is important to remark that the merging of the two inequivalent Dirac points and the opening of a gap, appear for a shear strain value $\zeta \approx 16\%$ which is lower than in the case of zigzag uniaxial deformation.¹⁴ The gap increases up to a maximum value of 0.72 eV for shear strain parameter of $\zeta \approx 20\%$, as shown in Fig. 4. We conclude that shear strain seems a likely candidate to achieve gap opening in graphene for a deformation far enough from failure strain and, therefore, achievable with no danger for the overall mechanical stability of the two-dimensional sheet.

Gap opening is predicted by the present TB calculation to occur at an even smaller strain parameter ζ , provided that a combination of shear and uniaxial strain is considered. By adding an uniaxial component to shear we generate a strain tensor of the form

$$\hat{\varepsilon} = \begin{pmatrix} \zeta & \zeta \\ \zeta & 0 \end{pmatrix} \quad \text{or} \quad \hat{\varepsilon} = \begin{pmatrix} 0 & \zeta \\ \zeta & \zeta \end{pmatrix} \quad (3)$$

for which the symmetry class of the lattice is not changed with respect to the pure shear case.

Nevertheless, uniaxial deformations along the armchair or zigzag direction are found to dissimilarly affect the band structure of graphene. Only in the last case we have observed the merging of the Dirac points already at $\zeta \approx 12\%$. The main features of the transition is the same as described before. The energy gap grows up to a maximum value of 0.95 eV (when the strain parameter achieves a value of $\zeta \approx 17\%$), reducing

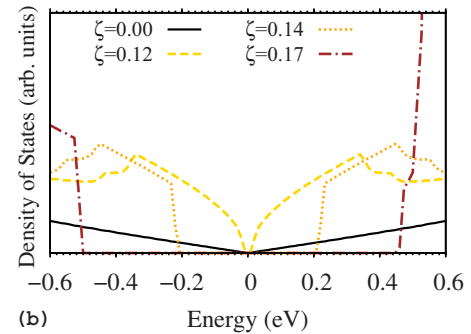
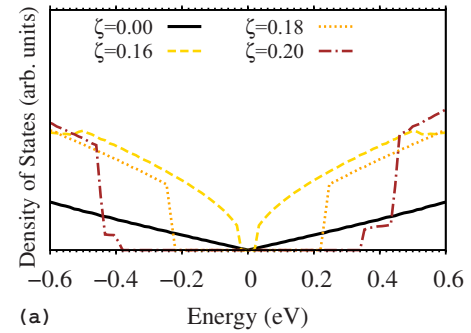


FIG. 5. (Color online) Density of states around the Fermi level (set conventionally at 0 eV) as function of the strain parameter ζ . Panel (a): graphene under pure shear deformation. Panel (b): graphene under combined shear and uniaxial deformation (along the armchair direction). The maximum value of the energy gap is observed for a strain parameter as large as $\zeta \approx 20\%$ and $\zeta \approx 17\%$, respectively.

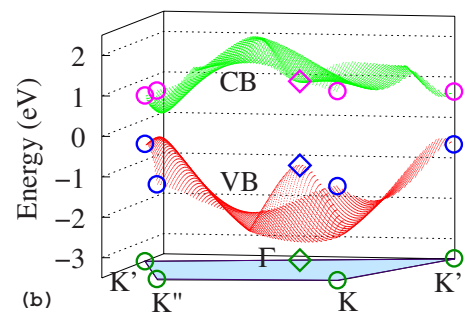
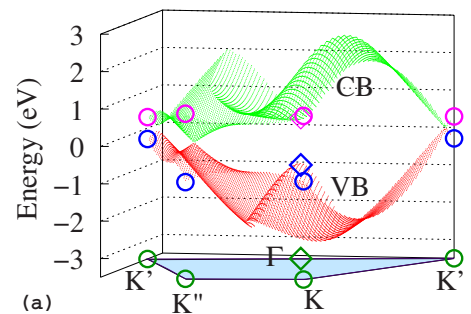


FIG. 6. (Color online) Top of the valence band (red, marked as VB) and bottom of the conduction band (green, marked as CB) of graphene under combined shear and uniaxial strain with $\zeta=15\%$. The uniaxial component of the strain is applied along the zigzag (panel a) and armchair (panel b) direction. Symbols connect the high-symmetry points of the BZ (bottom shaded area) to the energy of the corresponding electronic states.

again to zero at $\zeta \approx 20\%$ due to the steady decrease in the direct gap at Γ .

In order to quantitatively describe the evolution of the gap opening as function of the applied strain, the DOS has been calculated by a two-dimensional $75 \times 150 \times 1$ regular k -point mesh of the (deformed) BZ. As shown in Fig. 5, for a strain value less than 15% (panel a) or 11% (panel b), the DOS depends linearly on energy close to the Fermi level, showing a slope increasing with the strain. The two characteristic Van Hove singularities into the DOS move closer the Fermi energy and disappear into abrupt gap edges as soon as the gap is open. After the annihilation of the Dirac points, the DOS shows a $\sim \sqrt{E}$ behavior.

We conclude by remarking that the two strain contributions (i.e., uniaxial and shear) could be combined in different ways so as to modulate the energy-gap value. In Fig. 6, the electronic band structures of graphene under different combinations of shear and uniaxial strain are compared, keeping

the same value of the strain parameter $\zeta = 15\%$. While the combination of shear with uniaxial armchair shows a sizable energy gap of about 0.6 eV, the combination of shear with uniaxial zigzag is associated to a gapless band structure.

In conclusion, we have shown how the opening gap in the electronic spectrum of graphene could be achieved by applying deformations with a nonzero shear component, rather than a simple uniaxial deformation. Energy gaps have been found to vary in between 0.6 and 0.9 eV for a strain value far enough from failure. In particular, we have shown that the most effective way to control the gap opening is to combine a shear and an armchair uniaxial deformation.

We acknowledge computational support by CYBERSAR (Cagliari, Italy) and CASPUR (Rome, Italy). Discussions with G. Fadda are gratefully acknowledged. One of us (L.C.) acknowledges partial financial support by the MATHMAT project (Università di Padova, Italy).

*luciano.colombo@dsf.unica.it

- ¹K. S. Novoselov, A. K. Geim, S. V. Morozov, D. Jiang, Y. Zhang, S. V. Dubonos, I. V. Grigorieva, and A. A. Firsov, *Science* **306**, 666 (2004).
- ²A. H. Castro Neto, F. Guinea, N. M. R. Peres, K. S. Novoselov, and A. K. Geim, *Rev. Mod. Phys.* **81**, 109 (2009).
- ³K. S. Novoselov, Z. Jiang, Y. Zhang, S. V. Morozov, H. L. Stormer, U. Zeitler, J. C. Maan, G. S. Boebinger, P. Kim, and A. K. Geim, *Science* **315**, 1379 (2007).
- ⁴V. P. Gusynin and S. G. Sharapov, *Phys. Rev. Lett.* **95**, 146801 (2005).
- ⁵M. Y. Han, B. Özyilmaz, Y. Zhang, and P. Kim, *Phys. Rev. Lett.* **98**, 206805 (2007).
- ⁶F. Sols, F. Guinea, and A. H. Castro Neto, *Phys. Rev. Lett.* **99**, 166803 (2007).
- ⁷E. R. Mucciolo, A. H. Castro Neto, and C. H. Lewenkopf, *Phys. Rev. B* **79**, 075407 (2009).
- ⁸K. Nakada, M. Fujita, G. Dresselhaus, and M. S. Dresselhaus, *Phys. Rev. B* **54**, 17954 (1996).
- ⁹R. Balog, B. Jørgensen, L. Nilsson, M. Andersen, E. Rienks, M. Bianchi, M. Fanetti, E. Lægsgaard, A. Baraldi, S. Lizzit, Z. Sljivancanin, F. Besenbacher, B. Hammer, T. G. Pedersen, P. Hofmann, and L. Hornekær, *Nature (London)* **9**, 315 (2010).
- ¹⁰Z. H. Ni, H. M. Wang, Y. Ma, J. Kasim, Y. H. Wu, and Z. X. Shen, *ACS Nano* **2**, 1033 (2008).
- ¹¹P. Shemella and S. K. Nayak, *Appl. Phys. Lett.* **94**, 032101 (2009).
- ¹²K. S. Kim, Y. Zhao, H. Jang, S. Y. Lee, J. M. Kim, K. S. Kim, J. H. Ahn, P. Kim, J. Y. Choi, and B. H. Hong, *Nature (London)* **457**, 706 (2009).
- ¹³Z. H. Ni, T. Yu, Y. H. Lu, Y. Y. Wang, Y. P. Feng, and Z. X. Shen, *ACS Nano* **2**, 2301 (2008).
- ¹⁴V. M. Pereira, A. H. Castro Neto, and N. M. R. Peres, *Phys. Rev. B* **80**, 045401 (2009).
- ¹⁵C. Lee, X. Wei, J. W. Kysar, and J. Hone, *Science* **321**, 385 (2008).
- ¹⁶E. Cadelano, P. L. Palla, S. Giordano, and L. Colombo, *Phys. Rev. Lett.* **102**, 235502 (2009).
- ¹⁷V. M. Pereira and A. H. Castro Neto, *Phys. Rev. Lett.* **103**, 046801 (2009).
- ¹⁸G. Montambaux, F. Piéchon, J.-N. Fuchs, and M. O. Goerbig, *Phys. Rev. B* **80**, 153412 (2009).
- ¹⁹C. H. Xu, C. Z. Wang, C. T. Chan, and K. M. Ho, *J. Phys.: Condens. Matter* **4**, 6047 (1992).
- ²⁰E. Cadelano, S. Giordano, and L. Colombo, *Phys. Rev. B* **81**, 144105 (2010).
- ²¹G. Gui, J. Li, and J. Zhong, *Phys. Rev.* **78**, 075435 (2008).
- ²²By “merging” we mean the following: at a critical strain $\zeta \approx 15.95\%$ the Dirac points are so close that they annihilate in a single hybrid Dirac cone, which shows a peculiar energy-momentum dispersion: it is linear (quadratic) along (perpendicular) to the direction joining the two Dirac points. At $\zeta = 16.0\%$, a gap as small as 0.05 eV is eventually opened. More details about the motion of Dirac points in two-dimensional crystals under uniaxial stress are reported in Refs. 18, 23, and 24.
- ²³P. Dietl, F. Piéchon, and G. Montambaux, *Phys. Rev. Lett.* **100**, 236405 (2008).
- ²⁴Y. Hasegawa, R. Konno, H. Nakano, and M. Kohmoto, *Phys. Rev. B* **74**, 033413 (2006).